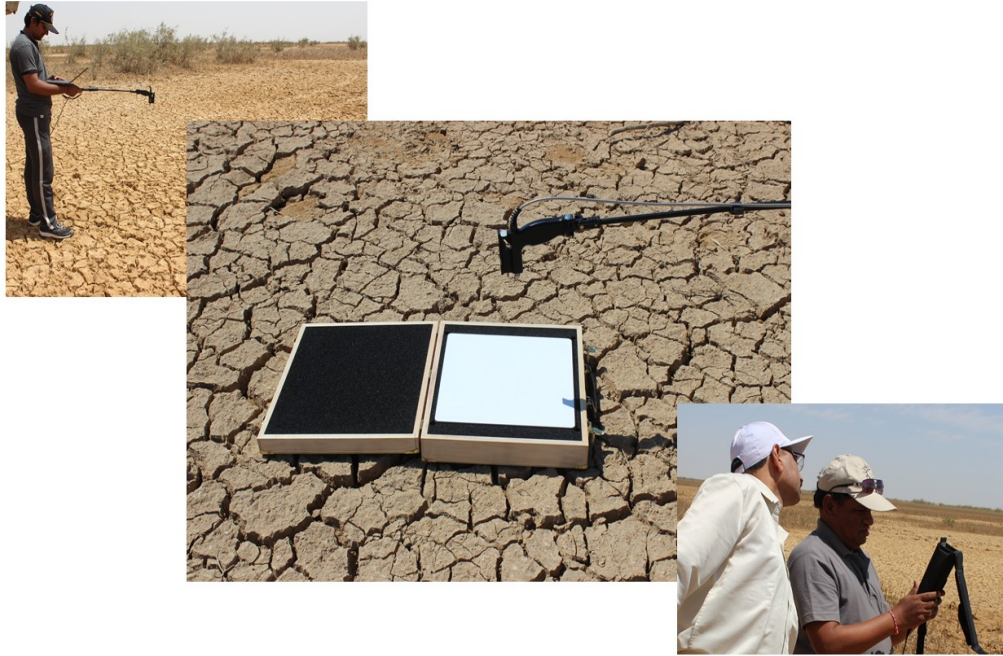


INSAT-3D Site Characterisation and calibration campaign in Great Rann of Kutchh

A Joint Campaign with India Meteorological Department



Earth-Ecosystem Research & Training Division (ERTD)
Earth, Ocean, Atmosphere, Planetary Sciences and Applications Area
Space Applications Centre (ISRO)
Ahmedabad
&
India Meteorological Department
Ministry of Earth Sciences
Delhi

July 2016

**Calibration and Validation Team of Joint Campaign in Great Rann of
Kutchh (19th April, 2016 - 23rd April, 2016)**

❖ **SAC-ISRO**

- 1) *Hiren Bhatt*
- 2) *R. P. Prajapati*
- 3) *Piyushkumar N Patel*
- 4) *BuddhiPrakash Jangid*

❖ **IMD-Delhi**

- 1) *Dr. A K Sharma*
- 2) *Dr. A K Mitra*
- 3) *Ms Shailesh Parihar*

❖ **IMD-Bhuj Office**

- 1) *Rakesh Kumar*
- 2) *Jagat Trivedi*
- 3) *Dr. Parul Trivedi*

Document control sheet

1. Report No.	SAC/EP SA/VRG/ERTD/01/2016
2. Publication Date	July, 2016
3. Title	INSAT-3D Site Characterisation and calibration campaign in Great Rann of Kutchh A Joint Campaign with India Meteorological Department
4. Type of Report	Scientific
5. Number of pages	22
6. Number of references	20
7. Authors	Hiren Bhatt, R. P. Prajapati, Piyush N. Patel, BuddhiPrakash Jangid, A.K.Sharma, A. K. Mitra, Shailesh Parihar, Rakesh Kumar, Japan Trivedi, Parul Trivedi
8. Originating unit	ERTD/VRG/EP SA
9. Abstract	This document describes the Site suitability for vicarious calibration of imager and over Great Rann of Kutchh.
10. Key Words	Vicarious Calibration, Radiative transfer code, Radiance at TOA
11. Security classification	Unrestricted
12. Distribution statement	Among all concerned

Table of Contents

1.	Abstract	1
2.	Introduction	1
3.	Site Characteristics	2
4.	Instruments and Measurements Strategy	4
5.	Measurements of Surface Reflectance	8
6.	Sunphotometer/Ozonemonitor Measurements	10
7.	Methodology	12
8.	Results and Discussion	14
9.	Estimation of Vicarious Calibration	16
10.	Conclusion	18
	Acknowledgement	19
	References	19

List of Figures

Figure 1: Location of calibration site at Bhuj in Great Rann of Kutchh	3
Figure 2: Marked points indicate the location where data are acquired during this field campaign. The different colours indicate the area covered for a particular day. Yellow (20-04-2016), Red (21-04-2016), Green (22-04-2016) and Blue (23-04-2016).	4
Figure 3: INSAT3D visible channel image (19th April, 2016, 10::00 IST/04:30 GMT) of clouds passing over Bhuj along with field photographs of clouds during 19th April, 2016.	5
Figure 4: Collection of surface reflectance using ASD hyper-spectral radiometer during the campaign.	6
Figure 5: Measurements of atmospheric parameters (aerosol optical depth, total columnar ozone and water vapour) using MicroTops-II sunphotometer and ozonemonitor during the campaign.	7
Figure 6: Daily averaged measured surface reflectance at Bhuj for all four clear-sky days in upper panel and Lower panel shows the standard deviation in the measured surface reflectance.	8
Figure 7: Image of the coefficient of variation calculated using 2km x 2km window in the two bands (VIS and SWIR) of the INSAT3D image acquired on GROK on 21st April, 2016 at 11:30 am. Red box shows the data collected site (4km x 4km).	9
Figure 8: Upper panel shows the variation of aerosol optical depth at five different wavelengths (340, 440, 500, 675 and 870 nm) and lower panel shows the variation in estimated Angstrom Exponent at 440-870 nm.	11
Figure 9: Upper panel shows the variation of Total columnar ozone in Dobson units and lower panel shows the variation of water vapor in cm measured using MicroTops-II ozonemonitor for all four clear-sky days.	12
Figure 10: Flow chart for the simulation of TOA radiance and estimation of calibration coefficient.	13
Figure 11: Pre-launch laboratory measurements of spectral response function for VIS and SWIR channels of INSAT-3D.	14
Figure 12: The combine linear regression between INSAT-3D measured and 6S simulated Radiance over GROK for Visible & SWIR channel for 2016.	15
Figure 13: The combine linear regression between INSAT-3D measured and 6S simulated Radiance over GROK for Visible & SWIR channel for 2015.	16
Figure 14: Estimated vicarious calibration gain coefficient over GROK Selected site.	17

Abstract

The objective of this document is to report the results of measurements carried out during the campaign of in-situ data collection for the vicarious calibration of INSAT3D imager and site characterisation near Bhuj in great Rann of Kutchh during 19th April, 2016 - 23rd April, 2016. The site selection and calibration campaign was carried out for Five consecutive days (19th April, to 23rd April, 2016, lost 19th data due to cloud) to account for characterization errors or undetermined post-launch changes in spectral response of the sensor. The measurements include surface reflectance using ASD Spectro-radiometer, aerosol, ozone and water vapour using MicroTops-II sunphotometer and ozonemonitor. This campaign is carried out with the joint collaboration of India Meteorological Department (IMD). The first objective is to understand the temporal and spectral stability of the selected site to be used for regular calibration of INSAT series of satellites. The second objective of these measurements is to perform the vicarious calibration for visible (VIS) and shortwave infrared (SWIR) channels of INSAT-3D imager over high-reflected target, and monitor the sensor performance since its launch in July 2013 and analyse the relative change in calibration coefficients if any since last calibration exercise in 2016.

1. Introduction

The technological advancement of satellite remote sensing data and usage of derived products for societal benefits not only requires the development of new and advanced satellites but also to improve the quality of its data products. Therefore, it has become very much essential to continuously monitor and update, if needed, the satellite sensor calibration throughout its mission life. In general, calibration procedure includes radiometric calibration (Bruegge et al., 1998) prior to launch, on-board calibration (Bruegge et al., 1993), and vicarious calibration using terrestrial targets. The post-launch sensor calibration exercises benefit the scientific communities to compensate the degradation owing to age and etc. (Rao, 2001), known as vicarious calibration. Vicarious calibration provides a method to absolute calibration of satellite sensors using reference and precise measurements of terrestrial targets' spectral reflectance from the

ground instruments. The selection of location / observation also to be looked for suitable site. This site should have higher reflectance (Bright), Approachable, Homogeneous, and radio metrically stable. Then the calibration co-efficient can be derived computing satellite measured and Ground measured and model derived radiance. This calibration co-efficients can be incorporated for the accurate in-orbit characterisation to convert the sensor raw digital counts to useful radiance values. Vicarious calibration is a broadly adopted technique for continuous monitoring of radiometric performance of satellite sensor, which involves the uncertainties computation in the calibration co-efficients to correct the radiometric response of the sensor (Thome et al., 1998). Vicarious calibration is performed through radiance simulation at sensor level using ground measured reflectance and atmospheric parameters under homogenous conditions. In all cases, the objective is traceability of data through calibration accuracies to the International System of Units (SI) for science users and data products with consistent quality for the broader user community.

This study details the measurements carried out for the purpose of vicarious calibration of visible (VIS) and shortwave infrared (SWIR) channels of INSAT-3D imager over Bhuj in great Rann of Kutchh with the collaboration of India Meteorological Department (IMD) during 19th April, 2016 to 23rd April, 2016.

2. Site Characteristics

Attributing to their preferable stability of surface characteristics and atmospheric dynamics, pseudo-invariant sites are commonly used for sensor radiometric calibration, degradation monitoring and inter-comparisons (Chandra et al., 2010; Bouvet et al., 2014) especially for the satellite sensors without on-board calibration facilities. The Committee on Earth Observation Satellites (CEOS) Working group on Calibration and Validation identified several sites around the world (Teillet and Chandra, 2010) based on the selection criteria, such as low probability of atmospheric interruptions, high spatial homogeneity, weak directional effects, flat reflectivity spectrum etc. Calibration sites are never chosen randomly, and to be adequate they must satisfy a certain number of criteria (Scott et al., 1996; Slater et al., 1996; Slater et al., 1987; Teillet et al., 1997).

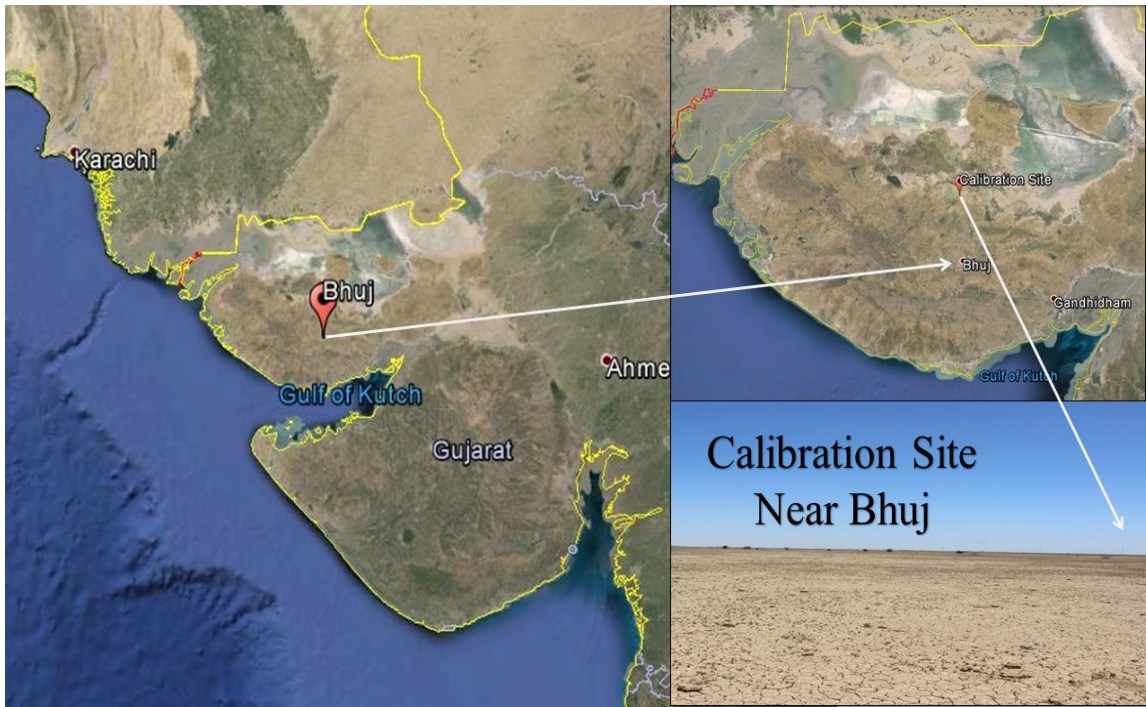


Figure 1: Location of calibration site at Bhuj in Great Rann of Kutchh (Courtesy Google Earth)

Initially, a joint campaign (Cal/Val team) was carried out in the month of February 26-28, 2015 to find a suitable site after visiting several locations in this region for the purpose of calibration and validation and to get the information of uniformity, accessibility, useable area and local information of the site. Based on the above criteria, we have selected a desert site in Great Rann of Kutchh (GROK), India (Figure-1, Courtesy Google-Earth).

Great Rann of Kutchh (GROK) site characterised as high and uniform reflectance land, was chosen to carry out vicarious calibration. The experimental site is placed about 40km away from Bhuj between Khawda and Loriya in Great Rann of Kutchh. The site is accessible near to road on the way to Khawda. The centre of the site used for calibration is located at 23.52185 °N and 69.65118 °E. The area of the site presents a smooth and homogenous surface characterized by a good spatial uniformity, which is used for radiometric calibration of sensors with large footprint e.g. INSAT3D imager. Figure-2 describes the points where data are acquired during this campaign (Courtesy Google-Earth).

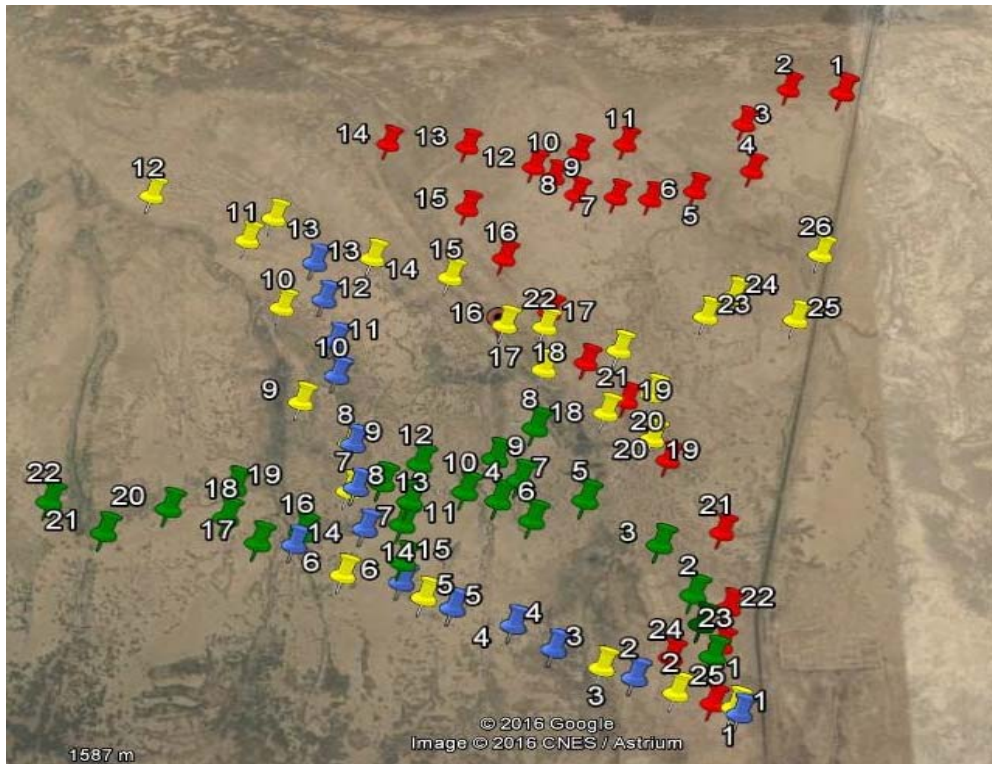


Figure 2: Marked points indicate the location where data are acquired during this field campaign. The different colours indicate the area covered for a particular day. Yellow (20-04-2016), Red (21-04-2016), Green (22-04-2016) and Blue (23-04-2016). (Courtesy Google Earth)

3. Instruments and Measurements Strategy

In the present campaign, several instruments are used for the in-situ data collection. Due to cloudy condition, we have avoided the first day of campaign (19th April, 2016) because clouds have major impact on radiance in the visible range. It is difficult to model the cloud in the radiative transfer model without in-situ observations of clouds. To avoid the uncertainty in vicarious calibration due to clouds, we abandoned the in-situ measurements of 19th April, 2016. Figure-3 shows the INSAT3D visible channel image of clouds passing over Bhuj along with filed photographs of clouds during 19th April, 2016 in Bhuj. To avoid atmospheric contamination, while modelling atmosphere we have limited our campaign only for the clear-sky days that were from 20th April, 2016 to 23rd April, 2016.

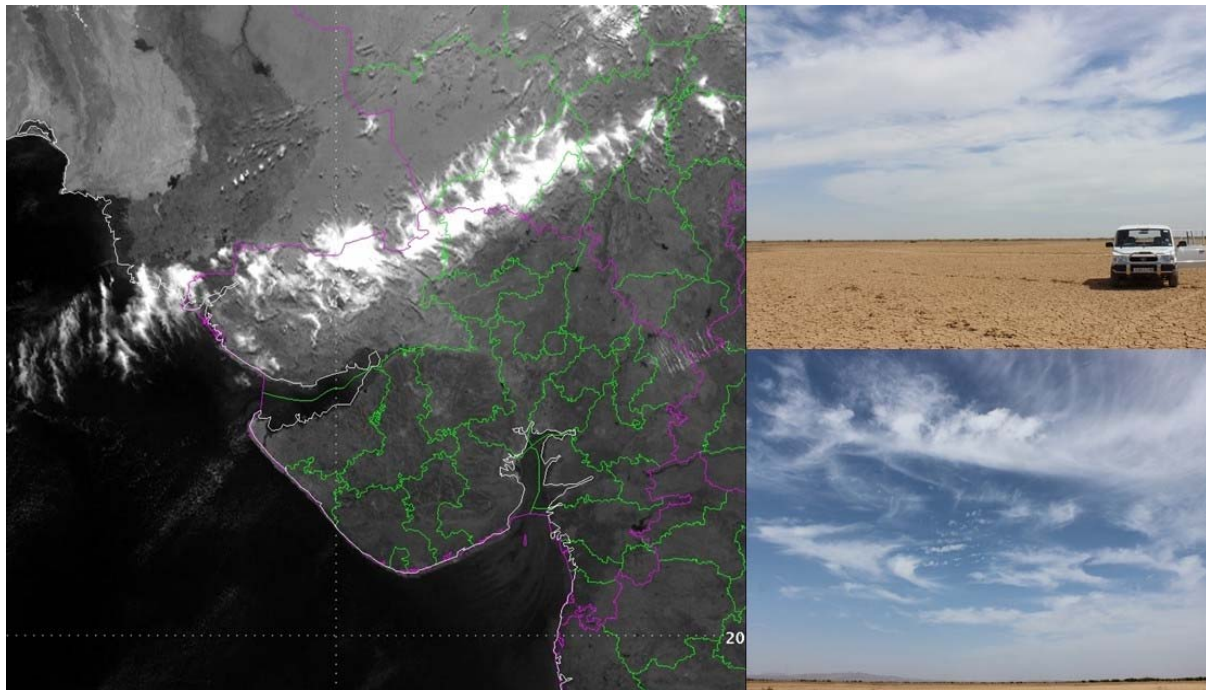


Figure 3: *INSAT3D visible channel image (19th April, 2016, 10::00 IST/04:30 GMT) of clouds passing over Bhuj along with field photographs of clouds during 19th April, 2016.*

Table-1 shows the list of instruments used for our objectives during the campaign of Bhuj. These instruments were operated according to its best measurement procedure and the measurement protocols (for the objective of Cal-Val exercise).

Table 1: *List of instruments used during Bhuj field campaign for data collection*

Instruments	Time period per day	Purpose
ASD Spectroradiometer	10:30 – 12:30	For the surface reflectance measurements
MicroTops-II Sunphotometer	10:30 – 12:30	For the aerosol optical depth measurements at five wavelengths
MicroTops-II Ozonemonitor	10:30 – 12:30	For the measurements of total columnar ozone and water vapour
Labsphere Spectralon reflectance panel	10:30 – 12:30	For the white reference measurements

Measurements of ground reflectance were carried out with a hyper-spectral radiometer (FieldSpec 3, Analytical Spectral Devices (ASD), Inc.), which covers the spectrum of measurements ranging from 350 to 2500 nm. Three spectrometers are

used to cover the full spectral-range. The first spectrometer uses a 512-element photo-diode array and a holographic reflective grating to cover the wavelength range from 350 to 1000nm. This spectrometer has a sampling interval of 1.4nm and the spectral resolution is 3nm at 700nm. Second and third spectrometers (SWIR1 and SWIR2) use a graded index InGaAs photo-diode to cover the wavelength ranges 1001-1800 nm and 1801-2500 nm, respectively. These have a sampling interval of 1.1 nm and the spectral resolution is 8 nm at 1400/2100 nm. A rapid data collection time of instrument is 0.1 second per spectrum and it operates with a fibre cable, 3 meter in length, with a 25° bare-optics field of view. Figure-4 shows the collection of surface reflectance using ASD hyper-spectral radiometer.



Figure 4: Collection of surface reflectance using ASD hyper-spectral radiometer during the campaign

The atmospheric aerosol optical depth (AOD) were derived from the measurements at multi wavelength (five different wavelengths, 380, 440, 500, 675 and 870 nm) Microtops-II sunphotometer (Solar Light Co., USA) of the solar instantaneous flux against its internal calibration using the Langley technique (Reagan et al. 1986;

Schmid and Wehli, 1995). The Full Width at Half Maximum (FWHM) bandwidth for the 380 nm channel is 2.4 ± 0.4 nm and 10 ± 1.5 nm for the other channels (Morys et al. 2001). Along with these instruments, a Microtops-II Ozonometer, a ground-based instrument, which is capable of measuring the total column ozone (TCO) using three UV channels (305.5, 312.5, 320.0 nm) and the total water vapour content (WVC) using two near-IR channels (940 and 1020 nm) (Porter et al. 2001) as well as AOD at 1020 nm was also deployed on all the seven days. Figure-5 describes the collection of atmospheric parameters using Microtops-II sunphotometer and ozonemonitor during the campaign.



Figure 5: Measurements of atmospheric parameters (aerosol optical depth, total columnar ozone and water vapour) using MicroTops-II sunphotometer and ozonemonitor during the campaign

Table-2 contains the daily variation of AOD at 500nm, TCO and WVC for all the seven days. More details of design, performance, error and calibration of Microtops-II is given elsewhere (Porter et al. 2001; Morys et al. 2001; Badarinath et al. 2007).

Table 2: Daily mean values of AOD at 500nm, Angstrom Exponent, Total Columnar Ozone in Dobson Unit (DU) and Water Vapour in cm.

Date	AOD at 500nm	Angstrom Exponent	Total Columnar ozone (DU)	Water Vapour (cm)	Date
20/04/2016	0.186	0.251	274.65	1.40	20/04/2016
21/04/2016	0.123	0.322	282.45	1.19	21/04/2016
22/04/2016	0.470	0.159	279.75	2.02	22/04/2016
23/04/2016	0.386	0.143	280.73	1.58	23/04/2016

4. Measurements of Surface Reflectance

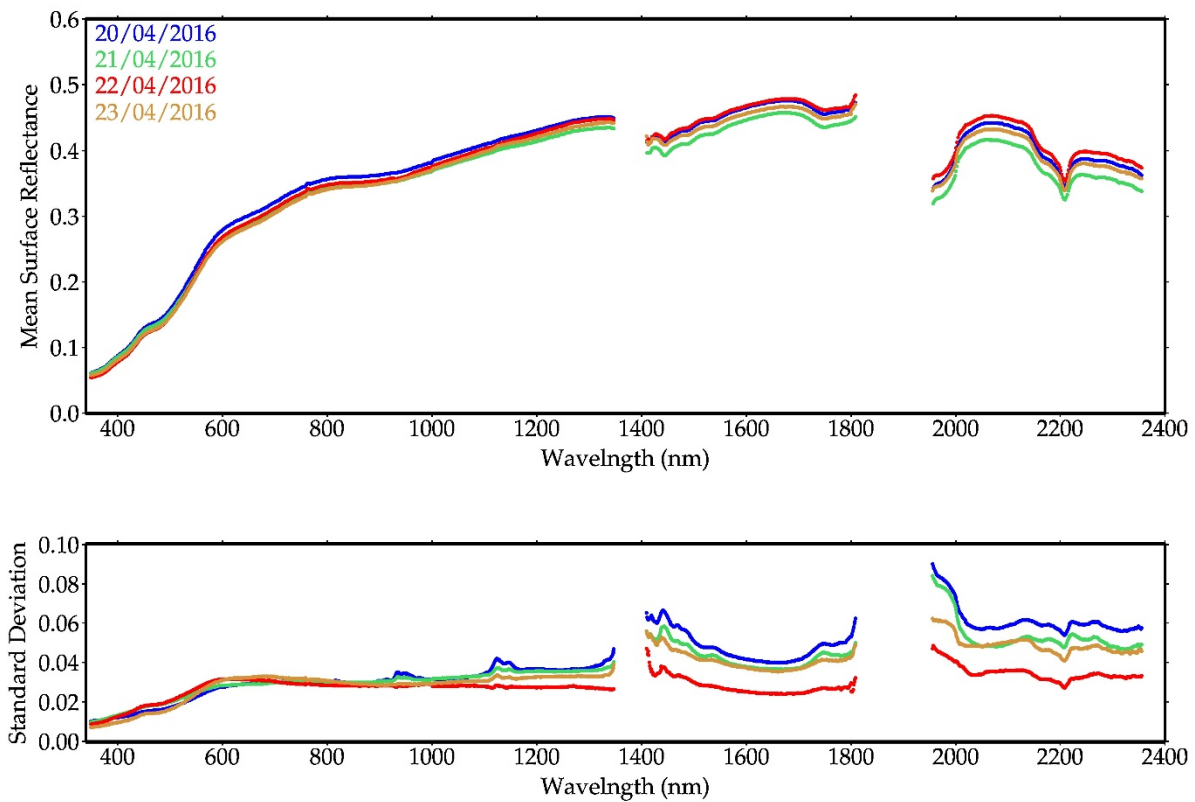


Figure 6: Daily averaged measured surface reflectance at GROK site for all four clear-sky days in upper panel and Lower panel shows the standard deviation in the measured surface reflectance

The FieldSpec Spectro-radiometer is specifically designed for field environment remote sensing to acquire visible-infrared (VNIR) and short-wave infrared (SWIR) spectra. This instrument is a compact, field portable, and precision instrument with a spectral range of 350-2500nm and were made between 10:30 IST/05:00 GMT and 12:30 IST/07:00 GMT for the measurements of field reflectance in the 4km x 4km region. Due to difficulty in accessibility of site, we have adopted the random approach for the data collection. However, the data are collected randomly within the site (4kmx4km) as shown in figure-2. The full site is covered once in these four days. We covered a site daily for 120 minutes to cover the 5 consecutive images (from 10:30 IST/05:00 GMT to 12:30 IST/07:00 GMT) of INSAT3D imager. Figure-6 illustrates the daily variation of surface reflectance for all four clear-sky days in the full spectral range in the upper panel along with standard deviation (at 1σ level) in the lower panel. Water vapour absorption at 1380nm and 1800nm are the major reasons for the two gaps in the reflectance curves. The standard deviation of the measured reflectance is observed to be 1%-2% in VIS (0.55-0.75 μ m) and SWIR (1.55-1.70 μ m) channels respectively, which indicates the spatial homogeneity of site.

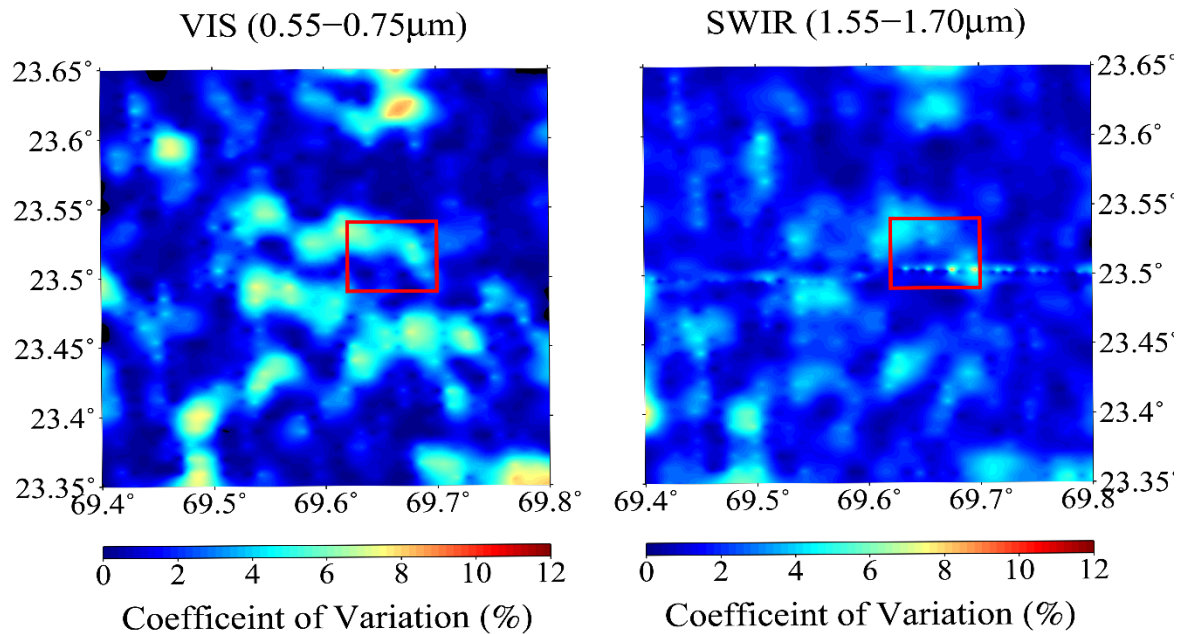


Figure 7: Image of the coefficient of variation calculated using 2km x 2km window in the two bands (VIS and SWIR) of the INSAT3D image acquired on GROK on 21st April, 2016 at 11:30 am. Red box shows the data collected site (4km x 4km)

Radiometric spatial uniformity and temporal stability of targets are main issues to consider when using target site for the calibration and long-term radiometric control of satellite sensor data (Bannari et al., 2005). The optical characteristics of any target site can vary due to topography variation, surface moisture variation, cracks in the dry surface that trap light, presence of vegetation, non-Lambertian behaviour of the surface increasing BRDF effects, as well as meteorological conditions. (Slater et al., 2004; Teillet et al., 1997; Thome et al., 2001). Radiometric spatial uniformity of the GROK site is confirmed by calculating spatial Coefficient of Variation (CV) measurements using cloud-free INSAT3D images over the site.

The image is acquired on 21st April, 2016 at 11:30 am. The study utilized VIS and SWIR bands. CV is defined by the ratio of the standard deviation over the average. In order to characterize the variability of the spatial homogeneity of the site, we set a 2 km x 2 km window size with a sampling step of 1 km. Figure-7 illustrates the result obtained using an INSAT3D image acquired on 21st April, 2016 at 11:30 am with the data collected site (4 km x 4 km) in red box. The CVs are found to be very similar for both the bands of INSAT3D imager. The highest values of CV are recorded 7.2% and 7.5% for VIS and SWIR, respectively, on the west side of the calibration site. The mean CV for the data collected site (red box) is found 5.1% and 4.2% for VIS and SWIR. This low variation indicates good site spatial homogeneity.

5. Sunphotometer/Ozonemonitor Measurements

Microtops-II sunphotometer and ozonemonitor are operated from 10:30 to 12:30Hrs with an interval of 10 minutes. The sunphotometer/Ozonometer have built-in processing capability to compute a variety of atmospheric parameters from instantaneous solar disk readings at several wavelengths. Table-2 contains the daily variation of AOD at 500nm, TCO and WVC for all four days.

The instrument pointing accuracy is very important in measuring these parameter using MicroTops-II unit as these equipment uses narrow field of view to point the Sun. The error due to miss-pointing is avoided through the concept of triplet measurement (the lowest value from triplet AOD has the maximum pointing accuracy), the lowest AOD value from a given triplet measurement is taken as valid while the Ozone and columnar

water vapour are averaged. AOD indicates the loading of aerosol in the atmosphere, where Angstrom exponent is a good indicator of the fraction of accumulation mode particles (radius < 1 μm) to coarse mode particles (radius > 1 μm) that describes the aerosol size distribution. Figure-8 illustrates the variation of aerosol optical depth at five channels (340, 440, 500, 675 and 870 nm) and estimated Angstrom exponent at 440-870nm over the region for all four clear-sky days.

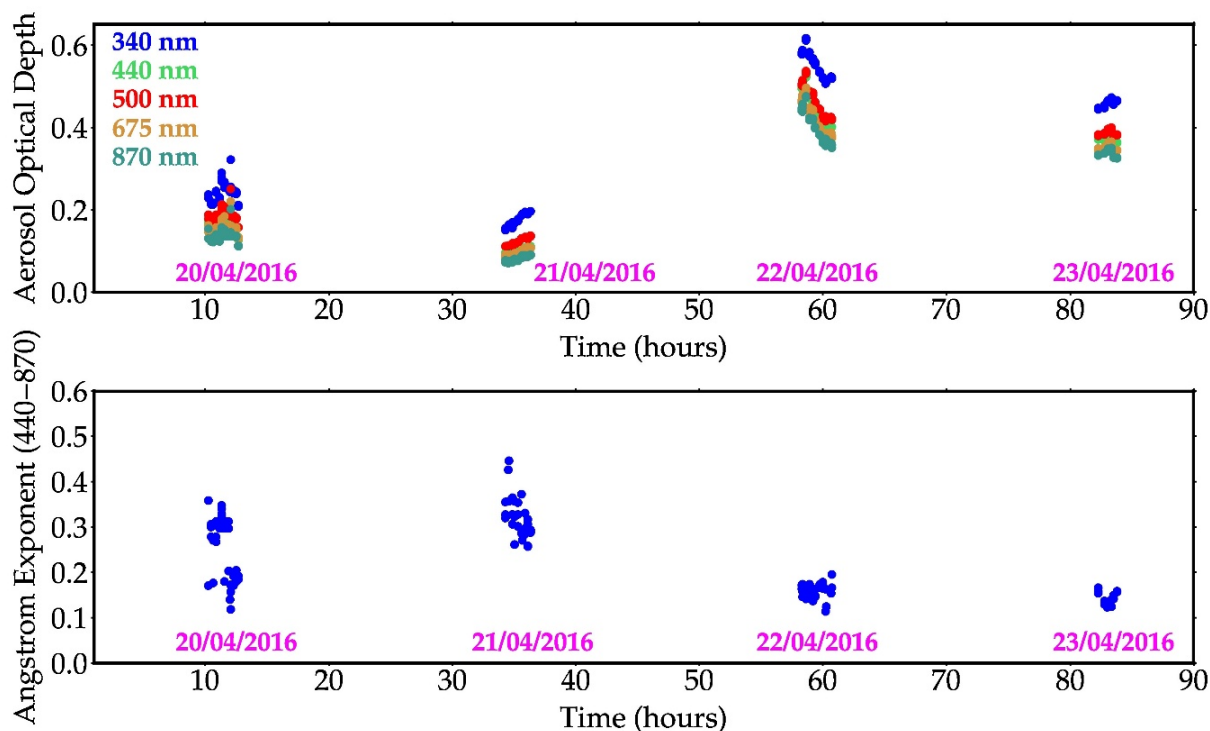


Figure 8: Upper panel shows the variation of aerosol optical depth at five different wavelengths (340, 440, 500, 675 and 870 nm) and lower panel shows the variation in estimated Angstrom Exponent at 440-870 nm

The measurements of total columnar ozone in Dobson units and water vapour in cm are carried out using MicroTops-II ozonemonitor. Figure-9 shows the time series variation of total columnar ozone and water vapour for all four days. The measurements details, procedure and the parameters measured using ASD hyper spectral-radiometer and MicroTops-II units (for the measurements of aerosol optical depth, total columnar ozone and water vapour). The measurements of atmospheric parameters determine stability of atmosphere and the site that helps us to model the atmospheric path radiance in radiative transfer model during vicarious calibration.

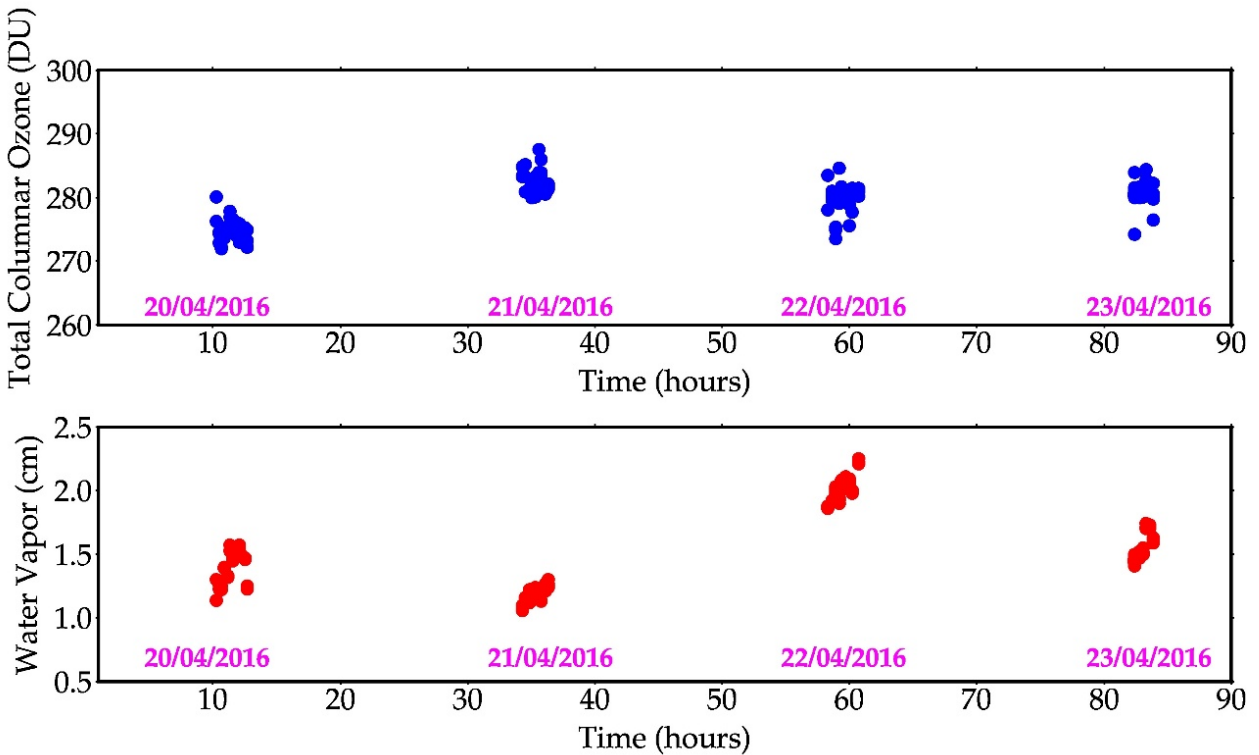


Figure 9: Upper panel shows the variation of Total columnar ozone in Dobson units and lower panel shows the variation of water vapour in cm measured using MicroTops-II ozonemonitor for all four clear-sky days

6. Methodology

In this study, vicarious calibration was performed using reflectance based approach, which was provided by Slater et al., (1987). This technique has been successfully used for satellite's sensor calibration (Biggar et al., 1991; Gellaman et al., 1993). In this technique, the INSAT-3D imager derived radiance is compared with 6S simulated TOA radiance. The vicarious radiometric calibration depends on measuring the surface reflectance, path from the sun to earth's surface and earth's surface to sensor and atmospheric optical thickness over a calibration site at the time of satellite overpass. These measurements are used as an input for RT code to simulate an absolute radiance at the sensor level. The field measurements are used to define the spectral directional reflectance of the surface and the spectral optical depth that are used to describe the aerosol and molecular scattering effect in the atmosphere (Gellman et al., 1991) and along with this we used columnar water vapour

include the water vapour absorption effect. The detailed values of atmospheric parameters are given in Table-2.

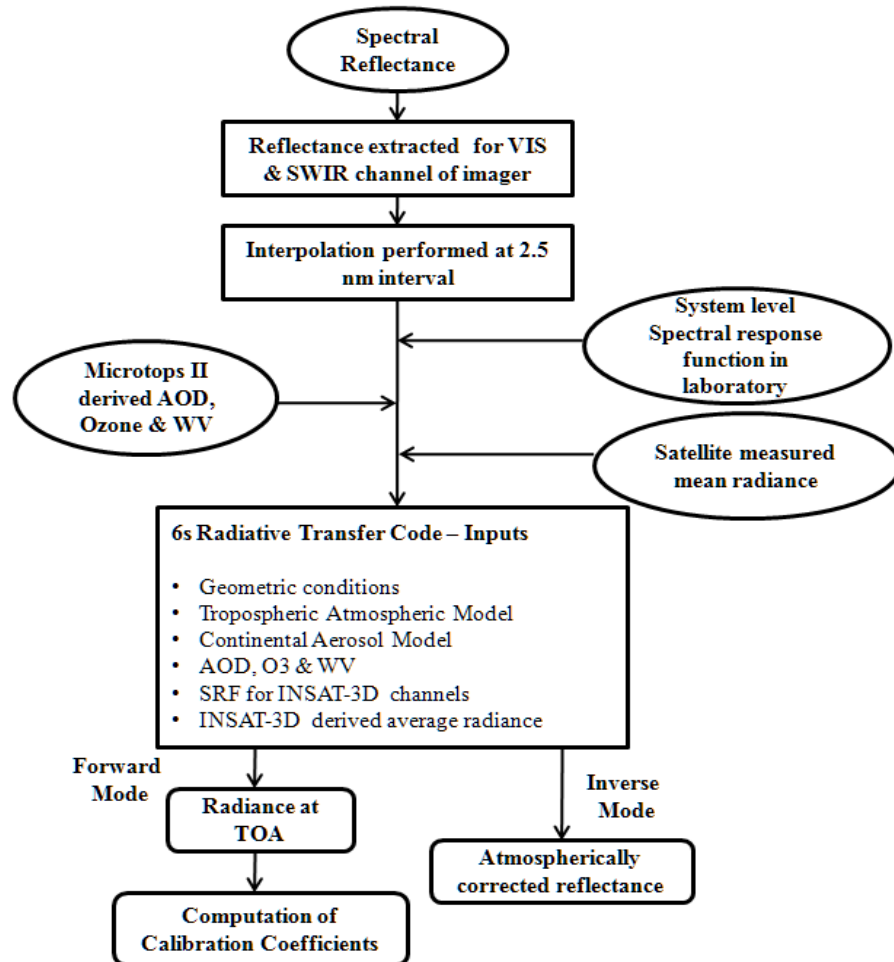


Figure 10: Flow chart for the simulation of TOA radiance and estimation of calibration coefficient

We have used 6S RT code to compute the radiance using ground measurements, which predicts the satellite signal at TOA level using field measurements. 6S RT model is a physically based model, not specified for particular satellite. In addition, 6S RT model utilizes gaseous absorption and scattering by aerosols and molecules. 6S performs better for atmospheric scattering as compared to other RT models (Markham et al., 1992). 6S model was formulated for the atmospheric correction in the short wavelengths. Figure 5 describes the flow chart to simulate radiance at TOA and vicarious calibration coefficient. The US 62 standard atmosphere profile provides the profiles of water vapour, ozone, pressure and

temperature up to 100km, at discrete intervals of 34 layers in the 6S RT model (Vermote et al., 2006).

Continental aerosol model is the basic model over the land site and it is assumed that there is no impact of marine and polluted urban aerosols over both the sites. The aerosol data with continental aerosol model were used as an input of 6S RT code. We have used pre-launch laboratory measurements of spectral response function as an input, which is shown in figure-11 (Murali and Padmanabhan, 2011). Both the SRF and ground reflectance data are resampled using spline interpolation method.

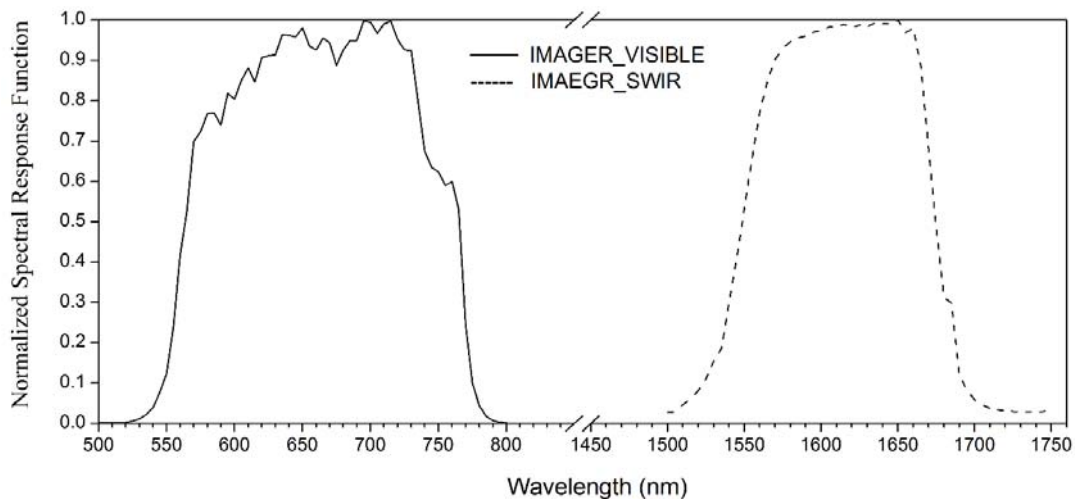


Figure 11: Pre-launch laboratory measurements of spectral response function for VIS and SWIR channels of INSAT-3D

6S RT model provides an output in the form of TOA radiance, which is divided by the corresponding radiance observed by the INSAT-3D imager to yield vicarious calibration coefficients.

7. Results and Discussion

The 6S simulated TOA radiance was compared with the INSAT-3D imager radiance. Table 3 describes the statistical parameters of regression analysis. As mentioned in earlier part of report the first date of observation was cloudy, so only four days observations were available. Finally total of 44 observation pixels are available which is a good number being used for computation. The result of combined linear regression along with daily linear regression for VIS and SWIR over GROK are shown in figure 12. The good statistical agreement was observed between satellite-derived radiance and

simulated radiance, with R^2 value of 0.96 with RMSE of $1.08 \text{ Wm}^{-2}\text{sr}^{-1}\mu\text{m}^{-1}$ for visible channel and R^2 value of 0.94 and RMSE of $0.28 \text{ Wm}^{-2}\text{sr}^{-1}\mu\text{m}^{-1}$ for SWIR channel of INSAT-3D Imager sensor.

Table 3: Summary of Statistics for regression analysis

Channels	NP	R^2	Bias	RMSE
VIS (0.55-0.75 μm)	44	0.96	1.31 $\text{Wm}^{-2}\text{sr}^{-1}\mu\text{m}^{-1}$	1.08 $\text{Wm}^{-2}\text{sr}^{-1}\mu\text{m}^{-1}$
SWIR (1.55-1.70 μm)	44	0.94	0.64 $\text{Wm}^{-2}\text{sr}^{-1}\mu\text{m}^{-1}$	0.28 $\text{Wm}^{-2}\text{sr}^{-1}\mu\text{m}^{-1}$

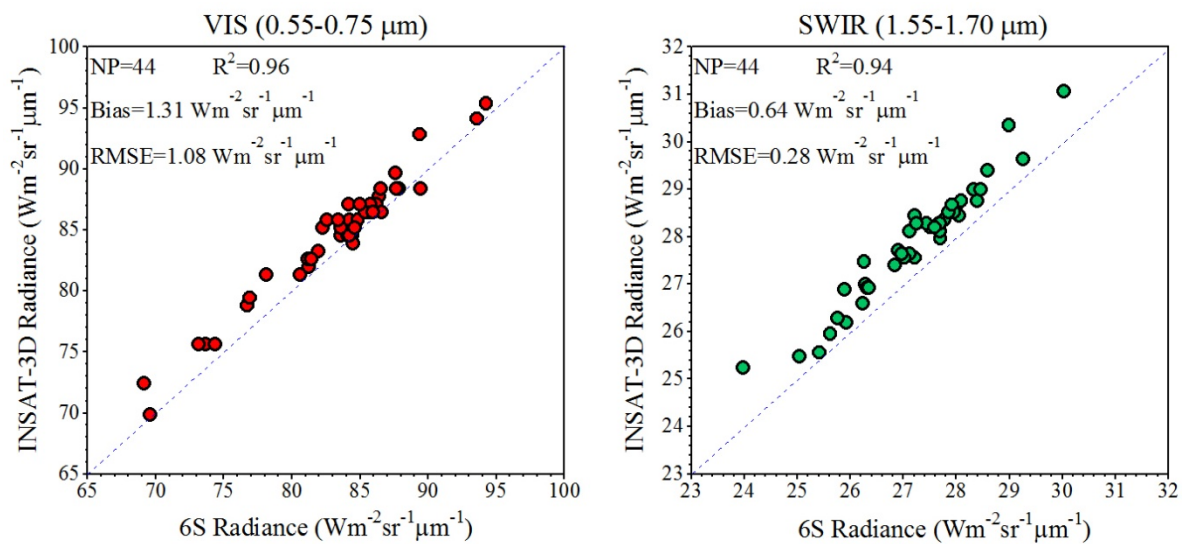


Figure 12: The combine linear regression between INSAT-3D measured and 6S simulated Radiance over GROK for Visible & SWIR channel for Year 2016

The bias between satellite-derived radiance and 6S simulated radiance is minimal, with the values of $1.31 \text{ Wm}^{-2}\text{sr}^{-1}\mu\text{m}^{-1}$ and $0.64 \text{ Wm}^{-2}\text{sr}^{-1}\mu\text{m}^{-1}$ for Visible and SWIR channels respectively.

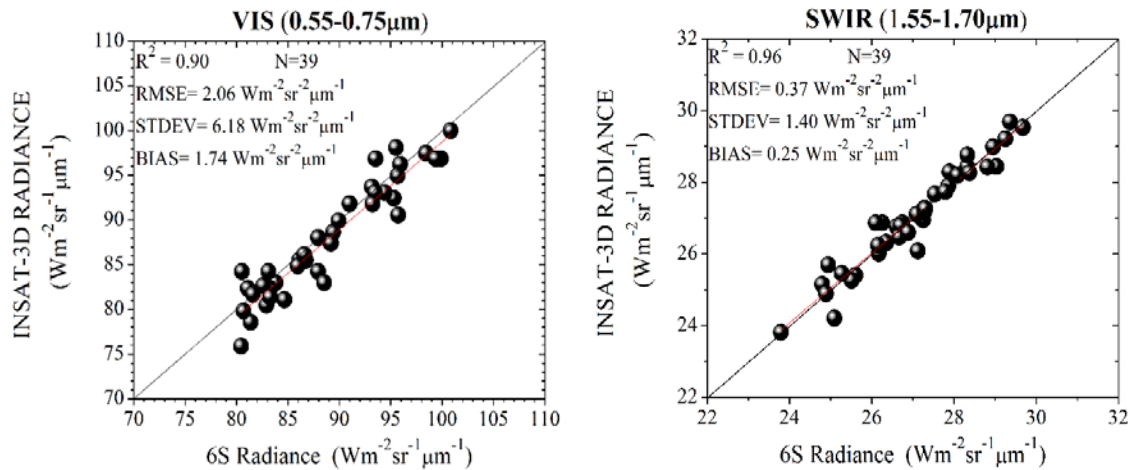


Figure 13: The combine linear regression between INSAT-3D measured and 6S simulated Radiance over GROK for Visible & SWIR channel for Year 2015

The result of combined linear regression along with daily linear regression for VIS and SWIR over GROK for Year 2015(Hiren et al 2015) are shown in figure 13. The good statistical agreement was observed between satellite-derived radiance and simulated radiance, with R^2 values of 0.90 and 0.97 and with RMSE values of $2.06 \text{ Wm}^{-2}\text{sr}^{-1}\mu\text{m}^{-1}$ and $0.37 \text{ Wm} \text{ Wm}^{-2}\text{sr}^{-1}\mu\text{m}^{-1}$ for Visible and SWIR channels respectively. The bias between satellite-derived radiance and 6S simulated radiance is minimal, with the values of $1.74 \text{ Wm}^{-2}\text{sr}^{-1}\mu\text{m}^{-1}$ and $0.25 \text{ Wm}^{-2}\text{sr}^{-1}\mu\text{m}^{-1}$ for VIS and SWIR channels respectively.

Hence it can be concluded that site is stable in time line and has consistency from year to year as far as radiometric properties are concerned.

8. Estimation of Vicarious Calibration

Table-4 describes the mean Top of Atmosphere radiance from satellite, Measured Radiance derived by 6s Simulation, and vicarious calibration coefficient derived from measurements at the GROK site for the study period. From table- 4, the mean values of simulated and satellite observed radiance are highly comparable throughout the two channels of INSAT-3D imager. The differences between simulated and observed radiance are very small which is due to the intrinsic variability and minor meteorological

variability of the sites. It was observed that radiance values for the SWIR channels are more comparable than visible channel.

Table 4: The values of radiance from INSAT-3D and 6S along with relative error and calibration coefficients for both the channels (VIS and SWIR) for all Four days of observation over GROK selected site

Date Of Observation	Channels	INSAT-3D Radiance ($Wm^{-2}sr^{-1}\mu m^{-1}$)	6S Simulated Radiance ($Wm^{-2}sr^{-1}\mu m^{-1}$)	Relative Error in Radiance Percentage (%)	Calibration Coefficient
20 th April 2016	VIS	84.84	83.35	-1.75	0.982
	SWIR	28.04	27.49	-1.92	0.980
21 st April 2016	VIS	85.49	84.23	-1.47	0.987
	SWIR	28.22	27.37	-3.03	0.970
22 nd April 2016	VIS	83.77	82.68	-1.29	0.986
	SWIR	27.56	26.97	-2.15	0.978
23 rd April 2016	VIS	83.42	81.85	-1.89	0.981
	SWIR	27.63	26.94	-2.50	0.975

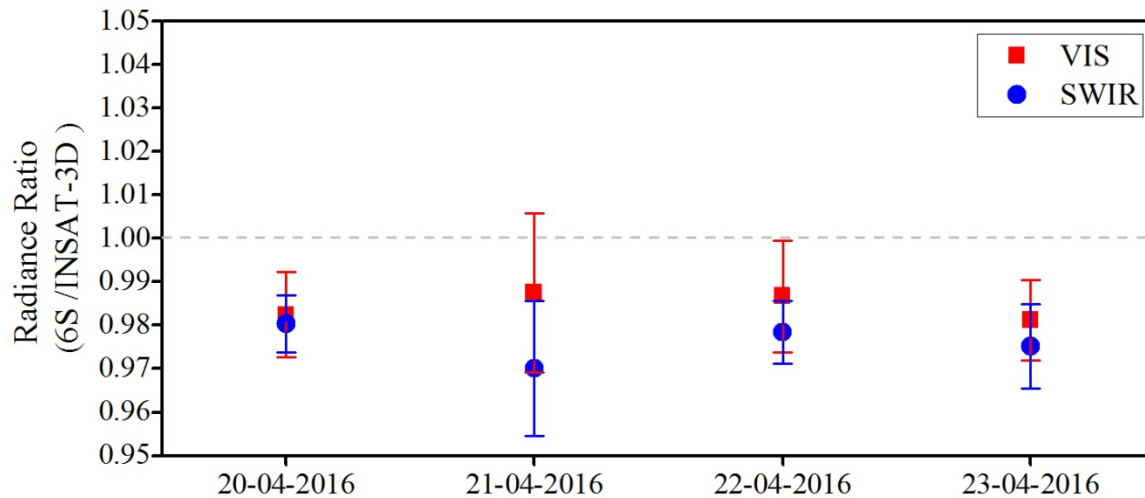


Figure 14: Estimated vicarious calibration gain coefficient over GROK Selected site

The vicarious calibration coefficient is the ratio of 6S simulated radiance and satellite observed radiance in the case of INSAT-3D imager. For an ideal case, if there is no degradation in the sensor during launch and ground and atmosphere are absolutely characterized and have an accurate RT code, simulated TOA radiance should precisely match with satellite observed radiance. It means the ratio of simulated to observe radiance should be unity. In practice it is not possible, there are uncertainties in field reflectance and atmospheric measurements, modelling uncertainties in the RT code.

Figure- 14 describes the ratio of the TOA radiance simulated using ground measured data to the INSAT-3D imager derived radiance for each channel and each day of observation along with average value. The vicarious calibration coefficient data for INSAT-3D imager describes minor changes in the calibration of INSAT-3D imager for both the channels and the change is slightly more in SWIR channel with respect to VIS. The standard deviation of the calibration coefficient is less than 3% for each channel in figure-13. This study aims towards the methodology followed and indicates that the errors (< 5%) lie within the radiometric uncertainty. The relative percentage error at both the channels for all days describes in Table-4. The relative errors are found to be less than 4%.

The relatively small biases in the VIS and SWIR channels are well in agreement with the INSAT-3D imager radiometric uncertainty. The noted values were found to be consistent, which indicate good calibration stability of INSAT-3D imager. The observations of calibration also show that the site is found suitable for calibration consistently.

9. Conclusion

In this study, post-launch calibration was carried out for the VIS and SWIR channels of INSAT-3D imager over the Great Rann of Kutchh and White Rann of Kutchh sites. The TOA radiance was simulated by 6S RT model using ground measurements. The conclusions based on this study are summarized below:

- 1) The present study concludes that GROK site is the preferred site for post-launch calibration due to its accessibility, high degree of homogeneity, Stability in terms of atmosphere radiometrically stable and brightness is also significant which helps to derive precise vicarious calibration coefficients.
- 2) The spatial and temporal variability of site is quantified by the variation of mean reflectance and coefficient of variation. The standard deviation of the measured reflectance is observed to be less than 3% in VIS (0.55-0.75 μ m) and SWIR (1.55-1.70 μ m) channels respectively, which indicates the spatial homogeneity of site.
- 3) The 6S simulated radiances are well comparable with the INSAT-3D imager measured radiance for all three dates of April 2015 and four dates of April 2016 over GROK site.
- 4) The close agreement was observed between simulated and satellite measured TOA radiance. The mean difference in vicarious calibration coefficients for the INSAT-3D imager measured radiance is slightly underestimated with respect to 6S radiance but the values are well within specifications of theoretical limits.
- 5) The results indicate that the observed Great Rann of Kutchh site can be recommended as suitable for Calibration and Validation activities of INSAT-3D and onward series of satellites.

Acknowledgement

The authors gratefully acknowledge the encouragement received from Director, SAC for carrying out the present research work. Valuable suggestions received from Deputy Director, EPSA, Group Head, VRG particularly during execution of study and inputs from Head CVD are also gratefully acknowledged.

References

Bruegge, C.J., Stiegman, A.E., Rainen, R.A., and Springsteen, A.W., 1993. Use of Spectralon as a diffuse reflectance standard for in-flight calibration of earth-orbiting sensors. *Optical Engineering*. 32, 805–814.

Bruegge, C.J., Duval, V.G., Chrien, N.L., Korechoff, R.P., Gaitley, B.J., and Hochberg, E.B., 1998. MISR prelaunch instrument calibration and characterization results. IEEE Transactions on Geoscience and Remote Sensing. 36, 1186–1198.

Rao, C.R.N., 2001. Implementation of the Post-Launch Vicarious Calibration of the GOES Imager Visible Channel. (Camp Springs, MD: NOAA Satellite and Information Services (NOAA/NESDIS)),
<http://www.ospo.noaa.gov/Operations/GOES/calibration/vicarious-calibration.html>.

Thome, K., Schiller, K.S., Conel, J., Arai, K., Tsuchida, S., 1998. Results of the 1997 Earth Observing System Vicarious Calibration joint campaign at Lunar Lake Playa, Nevada (USA). Metrologia. 35, 631–638.

Teillet, P. A. (1997). A status overview of Earth observation calibration/validation for terrestrial applications. Canadian Journal of Remote Sensing, 23 (4), 291-298.

Badarinath, K.V.S., Kharol, S.K., Kaskaoutis, D.G., and Kambezidis, H.D., 2007. Dust Storm over Indian Region and Its Impact on the Ground Reaching Solar Radiation—A Case Study Using Multi-satellite Data and Ground Measurements. Sci. Total Environ. 384, 316–332.

Morys, M., Mims III, F.M., Hagerup, S., Anderson, S.E., Baker, A., Kia, J., and Walkup, T., 2001. Design, calibration, and performance of MICROTOPS II handheld ozone monitor and Sun photometer. J. Geophys. Res. 106, D13, 14573–14582.

Porter, J.N., Miller, M., Pietras, C., and Motell, C., 2001. Ship-based Sun Photometer Measurements Using Microtops Sun Photo-meters. J. Atmos. Oceanic Technol. 18, 765–774.

Reagan, J.A., Thomason, L.W., Herman, B.M., and Palmer, J.M., 1986. Assessment of atmospheric limitations on the determination of the solar spectral constant from ground-based spectroradiometer measurements. IEEE – trans. Geosci. Remote Sensing. GE-24, 258-266.

Schmid, B., and Wehrli, C., 1995. Comparison of sun photometer calibration by use of the Langley technique and standard lamp. Appl. Opt. 34, 4500-4512.

Murali, K.R., and Padmanabhan, D., 2011. Spectral response details, INSAT-3D imager (FM)-V-2.0. Technical Report. SAC/EOSG/GPID/30/03/2011/17.

Chander, G., Xiong, X., Choi, T., and Angal, A., 2010. Monitoring on-orbit calibration stability of the Terra MODIS and Landsat 7 ETM+ sensors using pseudo-invariant test sites. *Remote Sensing of Environment*. 114, 925–939.

Teillet, P., and Chander, G., 2010. Terrestrial reference standard sites for post-launch sensor calibration. *Canadian Journal of Remote Sensing*. 36, 437–450.

Scott, K.P., Thome, K.J., and Brownlee, M., 1996. Evaluation of the railroad valley playa for use in vicarious calibration. *Proc. SPIE*. 2818, 158–166.

Slater, P.N., Biggar, S.F., Thome, K.J., Gellman, D.I., and Spyak, P.R., 1996. Vicarious radiometric calibrations of EOS sensors. *J. Atmos. Oceanic Technol.* 13, 349–359.

Slater, P.N., Biggar, S.F., Holm, R.A., Jackson, R.D., Mao, Y., Moran, M.S., Palmer, J.M., and Yuan, B., 1987. Reflectance-and radiance-based methods for in-flight absolute calibration of multispectral sensors. *Remote Sens. Environ.* 22, 11–37, 1987.

Bannari, A., Omari, K., Teillet, P.M., and Fedosejevs, G., 2005. Potential of Getis statistics to characterize the radiometric uniformity and stability of test sites used for the calibration of Earth observation sensors. *IEEE Transactions on Geoscience and Remote Sensing*. 43(12), 2918–2926.

Thome, K. I., Schiler, S., Conel, J., Arai, K., and Tsuchida, S., 1999. Results of the 1996 EOS Vicarious Calibration Joint Campaign at Lunar Lake Playa, Nevada, USA. *Metrologia*. 35, 631-638.

SAC- Hiren Bhatt, R P Prajapati, Piyush Patel , IMD-A.K.Sharma, A. K. Mitra, Rakesh Kumar, D. M. Hindia, and K. C. Modh “Calibration and Validation Site characterisation of INSAT-3D Satellite over Great Rann of Kutchh and White Rann of Kutchh”, Joint Campaign of SAC & IMD, SAC/EPASA/ADVG/CVD/CAL-VAL/SR/05/05/2015



Cal-Val Team members from SAC-ISRO and IMD (Delhi and Bhuj) during calibration campaign (19th April, 2016 - 23rd April, 2016) at Bhuj, Great Rann of Kutch.